PNAS

Supporting Information for

Holocene variations in Lake Titicaca water level and their implications for sociopolitical developments in the central Andes.

Stéphane Guédron *, Christophe Delaere, Sherilyn. C. Fritz, Julie Tolu, Pierre Sabatier, Anne-Lise Devel, Carlos Heredia, Claire Vérin, Eduardo Q. Alves, and Paul A. Baker.

*corresponding author: Stéphane Guédron
Email: stephane.guedron@ird.fr

This PDF file includes:

Supporting text
Figures S1 to S5
Tables S1 to S4
SI References

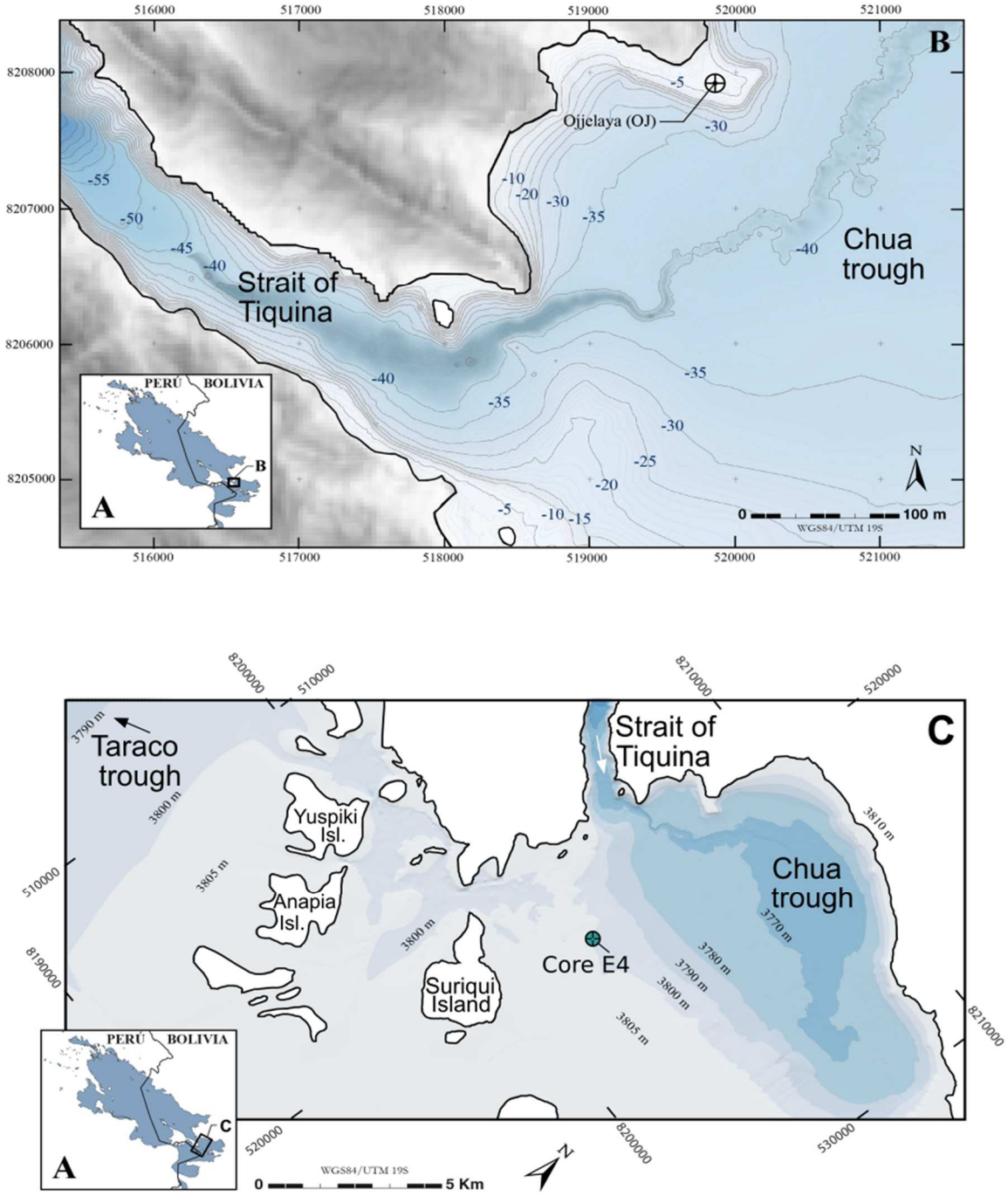

Fig. S1: Bathymetric maps obtained from survey performed between 2013 and 2018 with a multibeam echo-sounder Panoptix™ PS30 and GPSMAP®7410 (22). A) location of the zoom areas on the Lake Titicaca map at the connection between Lago Mayor and Lago Menor. B) Bathymetric map of the Strait of Tiquina, the connection between Lago Mayor and the Lago Menor, showing the channel incision likely originating from the flooding of the Lago Menor at the end of the Middle Holocene lowstand. The highest elevation of the deeper part of the Strait (pass) is reevaluated at 39.5 m depth below modern lake level (3810 masl). C) Bathymetric map of the outlet of the Strait of Tiquina showing i) the channel incision to the east toward the Chua trough with an average depth of 3770 masl (also shown in panel B), and ii) another incision to the west, flowing north of Suriqui Island, showing the most probable connection between the eastern (Chua trough) and western (Taraco trough) subbasin of Lago Menor. Sediment in this area has probably been covered by a turbidite recorded in core E4 (Fig. S3B) dated to the 18th century.

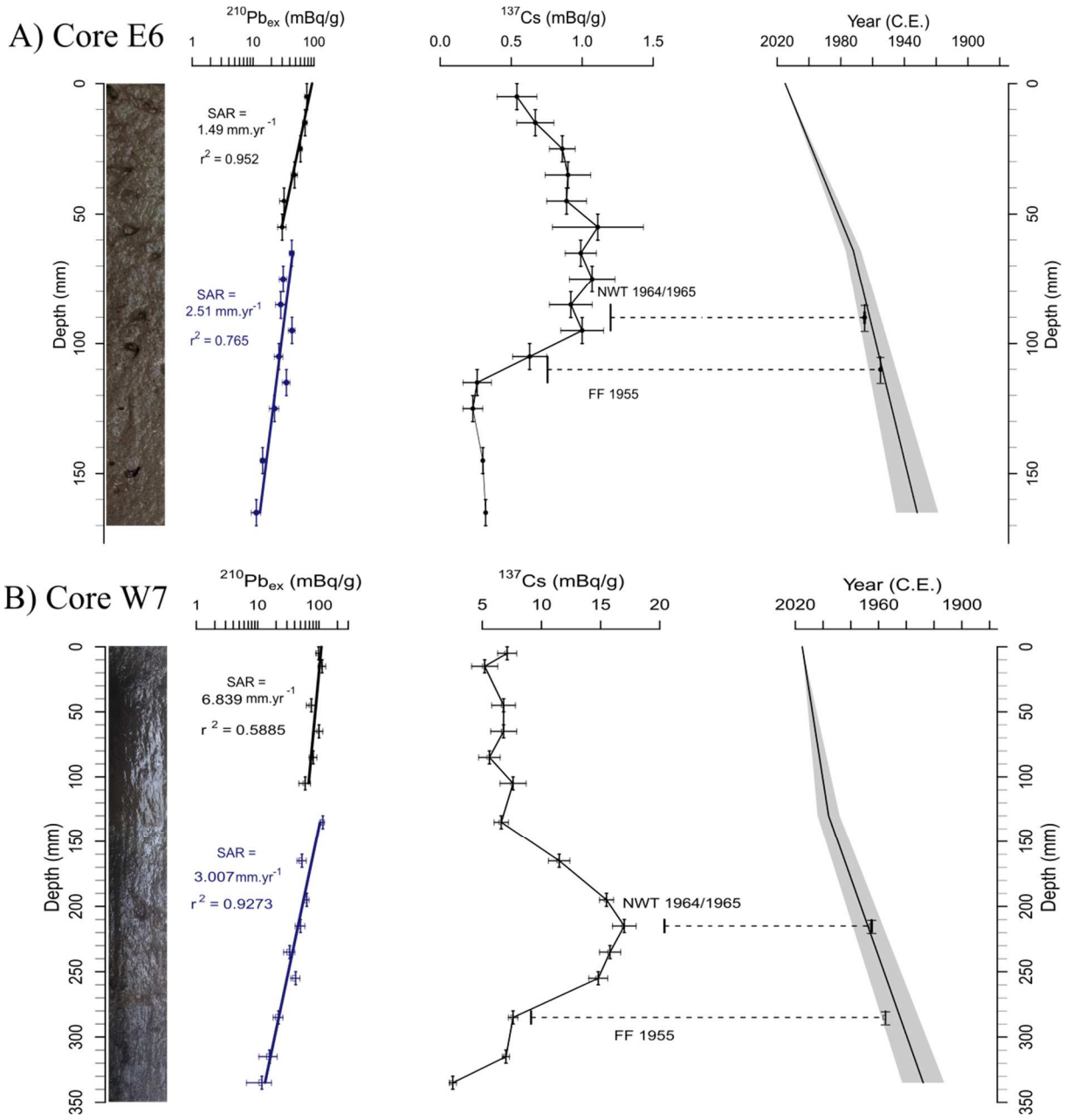

Figure S2A: $^{210}Pb_{ex}$ and ^{137}Cs depth profiles and CFCS Age - depth model for A) core E6 and B) core W7 collected in the eastern and western part of the southern Lake Titicaca subbasin (Lago Menor), respectively.

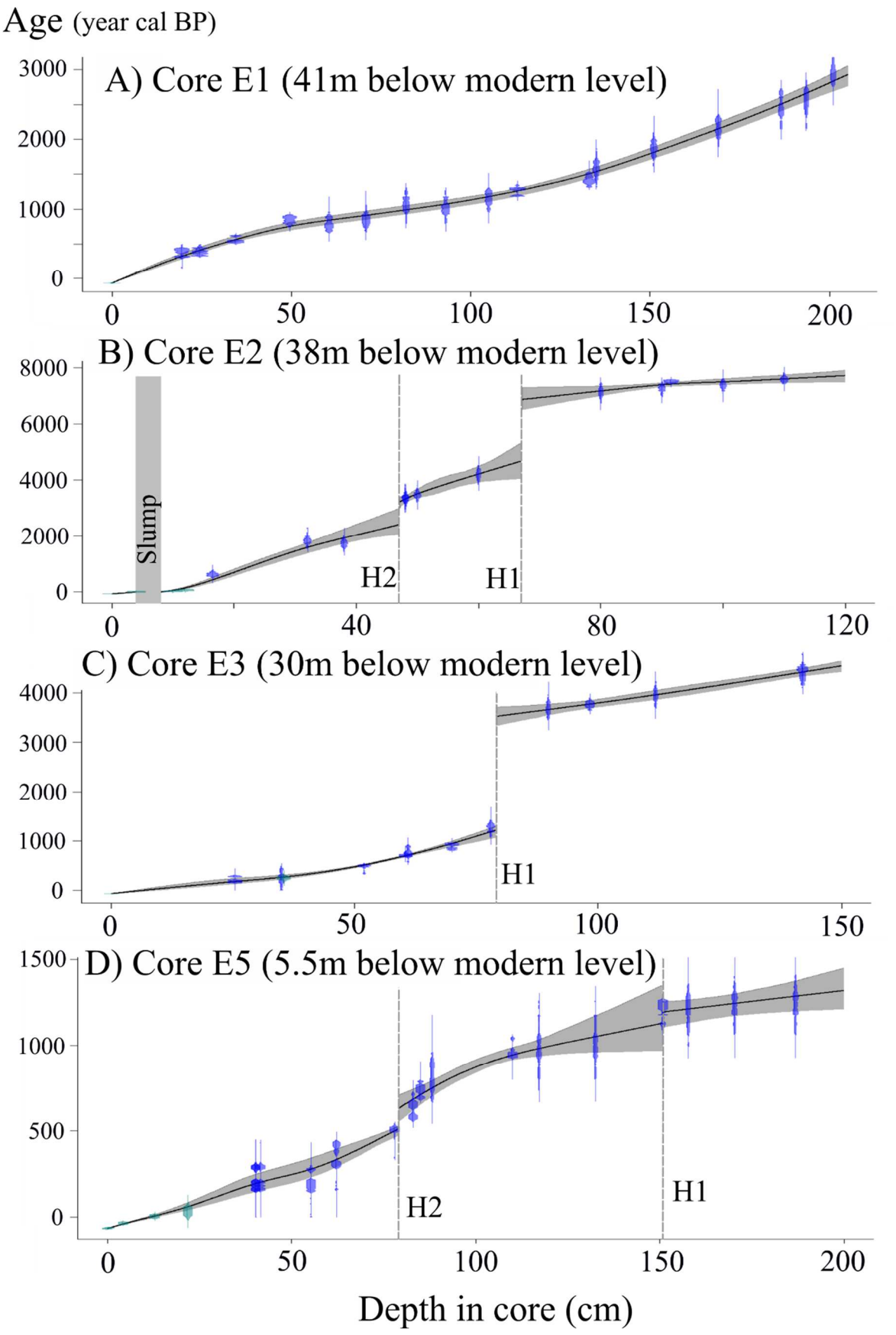

Figure S2B: Age Depth models for the four cores collected in the eastern part of the southern Lake Titicaca subbasin.

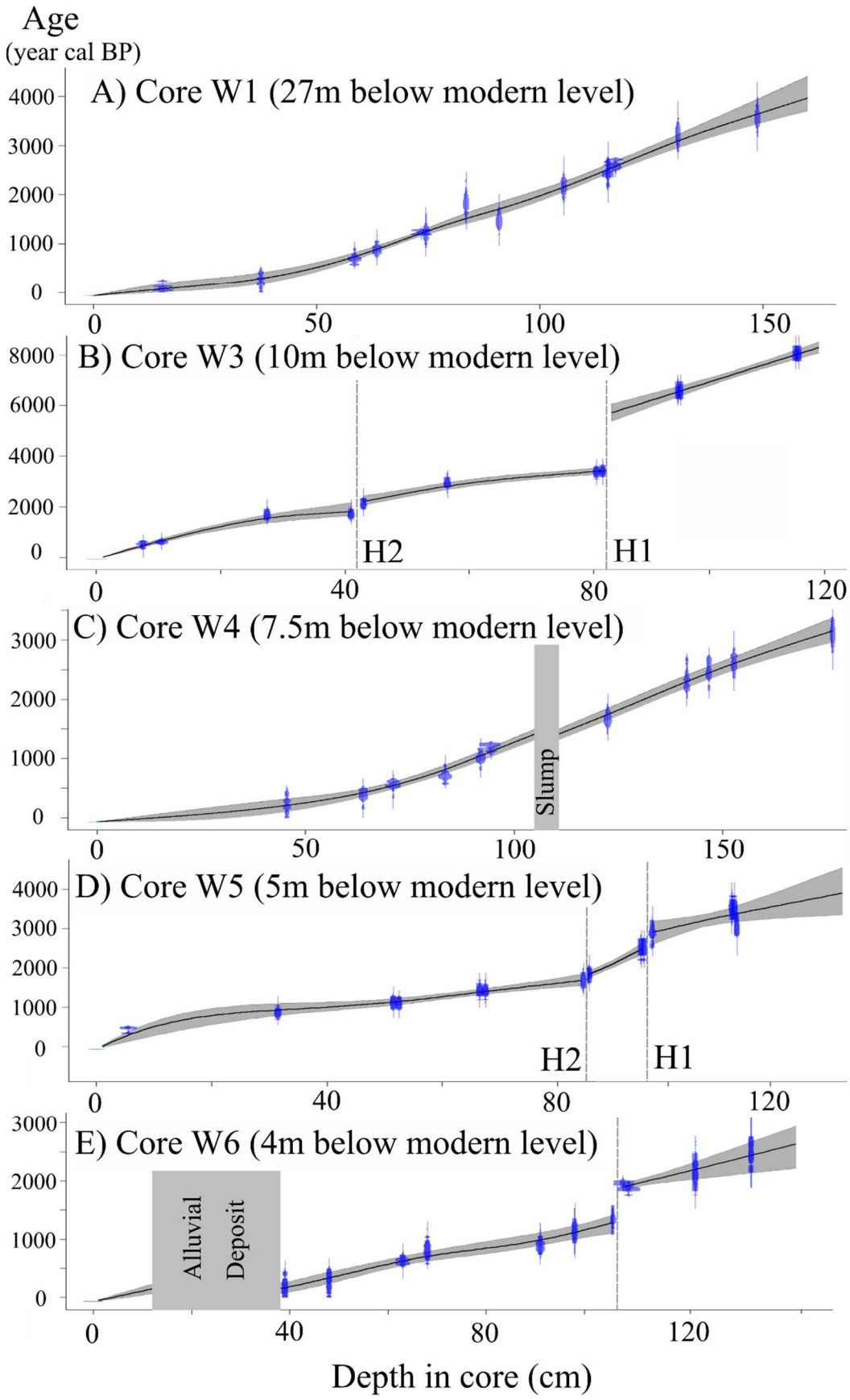

Figure S2C: Age Depth models for the five cores collected in the western part of the southern Lake Titicaca subbasin.

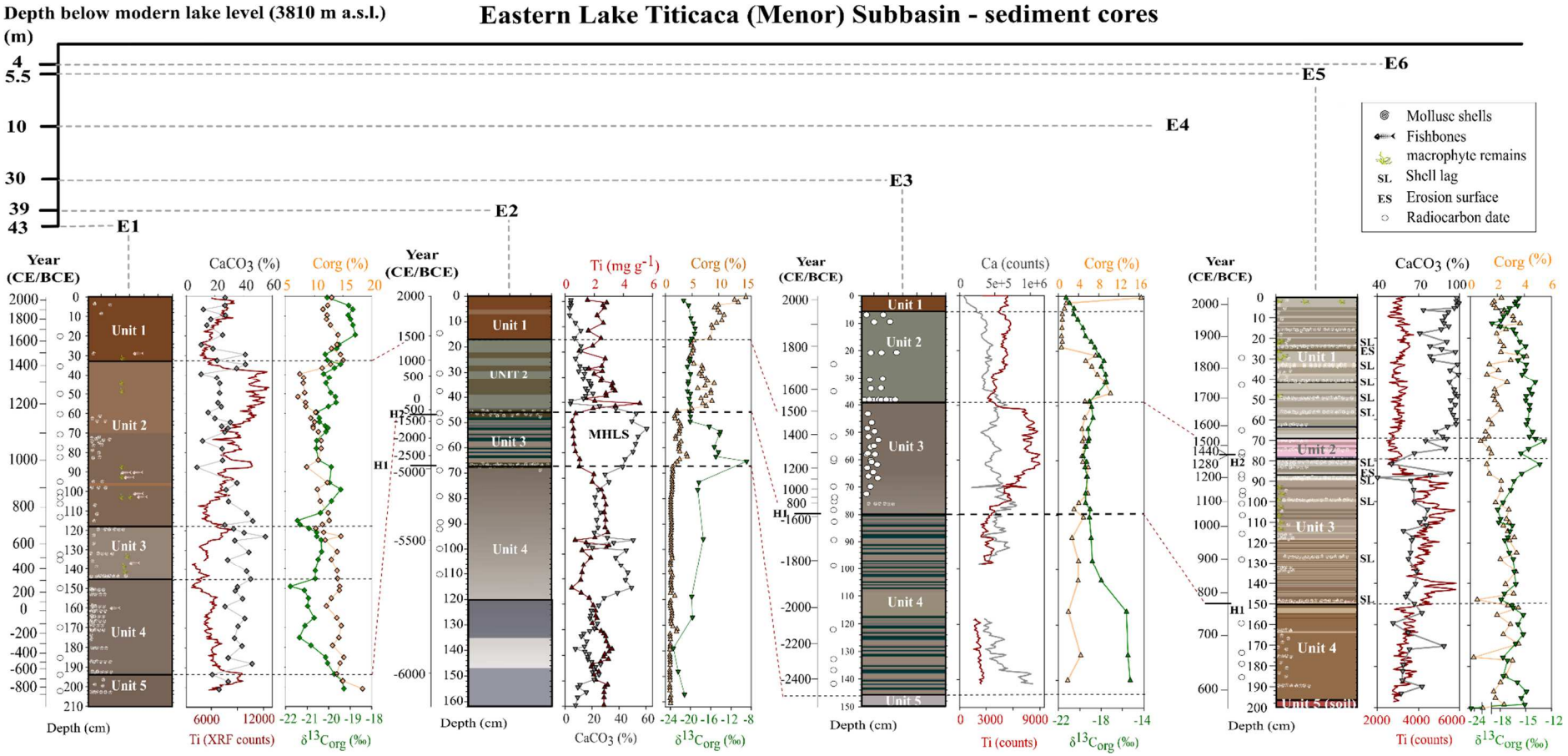

Fig. S3A: Sediment profiles from the eastern subbasin of Lago Menor with their lithology and depth profiles of Ca, Ti, C_{org} and $\delta^{13}C_{org}$ (uncorrected for the Suess effect). Lines indicate core scan XRF measurements, and symbols refer to chemical measurements. For shallow-water cores (E5 and E6) high $CaCO_3$ content and $\delta^{13}C_{org}$ values indicate a moderately shallow lake, where Characeae dominate the benthic area (> 2 m water depth), whereas low $CaCO_3$ and $\delta^{13}C_{org}$ values, but high C_{org} content indicate near-shore shallow-water environments (< 2m) where totora sedges dominate. The transition from carbonate-rich units with low $\delta^{13}C_{org}$ values to organic-rich facies in deep cores (E2 and E3) indicate an increase in lake level at the end of the Middle Holocene lowstand (MHLS) between 2500 and 1500 BCE. The thick deposits of organo-detrital and carbonate rich sediments in the shallow areas reflect a significant rise in water level during the 6th century (above the soil layer in core E5), followed by a second rise around the 16th century. The major transgression of the lake during the 6th century has certainly caused sedimentary erosion (H1 hiatus) on the steep slopes of the Chua trough (E2 and E3). The core from the bottom of the trough (E1) is not affected by this erosive phase and shows continuous and high sedimentation rates due to sediment focusing.

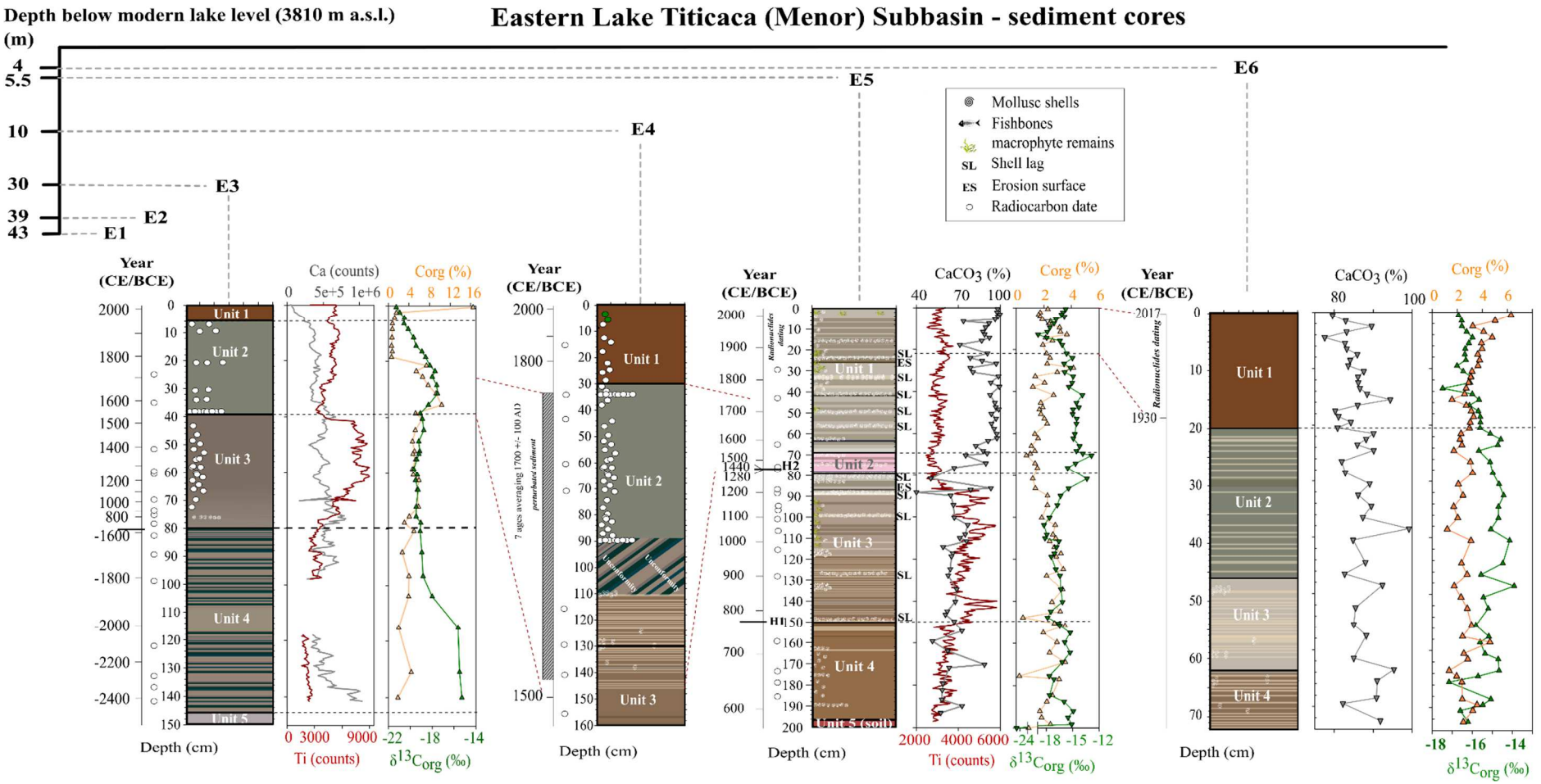

Fig. S3B: Sediment profiles from the eastern subbasin of Lago Menor with their lithology and depth profiles of Ca, Ti, C_{org}, and $\delta^{13}C_{org}$ (uncorrected for the Suess effect). Lines indicate core scan XRF measurements, and symbols refer to chemical measurements. For shallow-water cores (E5 and E6) high $CaCO_3$ content and $\delta^{13}C_{org}$ values indicate a moderately shallow lake, where Characeae dominate the benthic area (> 2 m water depth), whereas low $CaCO_3$ and $\delta^{13}C_{org}$ values, but high C_{org} content indicate near-shore shallow-water environments (< 2 m), where totora sedges dominate. The massive sediment deposit (~ 1m of sediment) in core E4 probably results from the erosion of the littoral zones (Siriqui island area) during the last major lake rise dated to the 16th century.

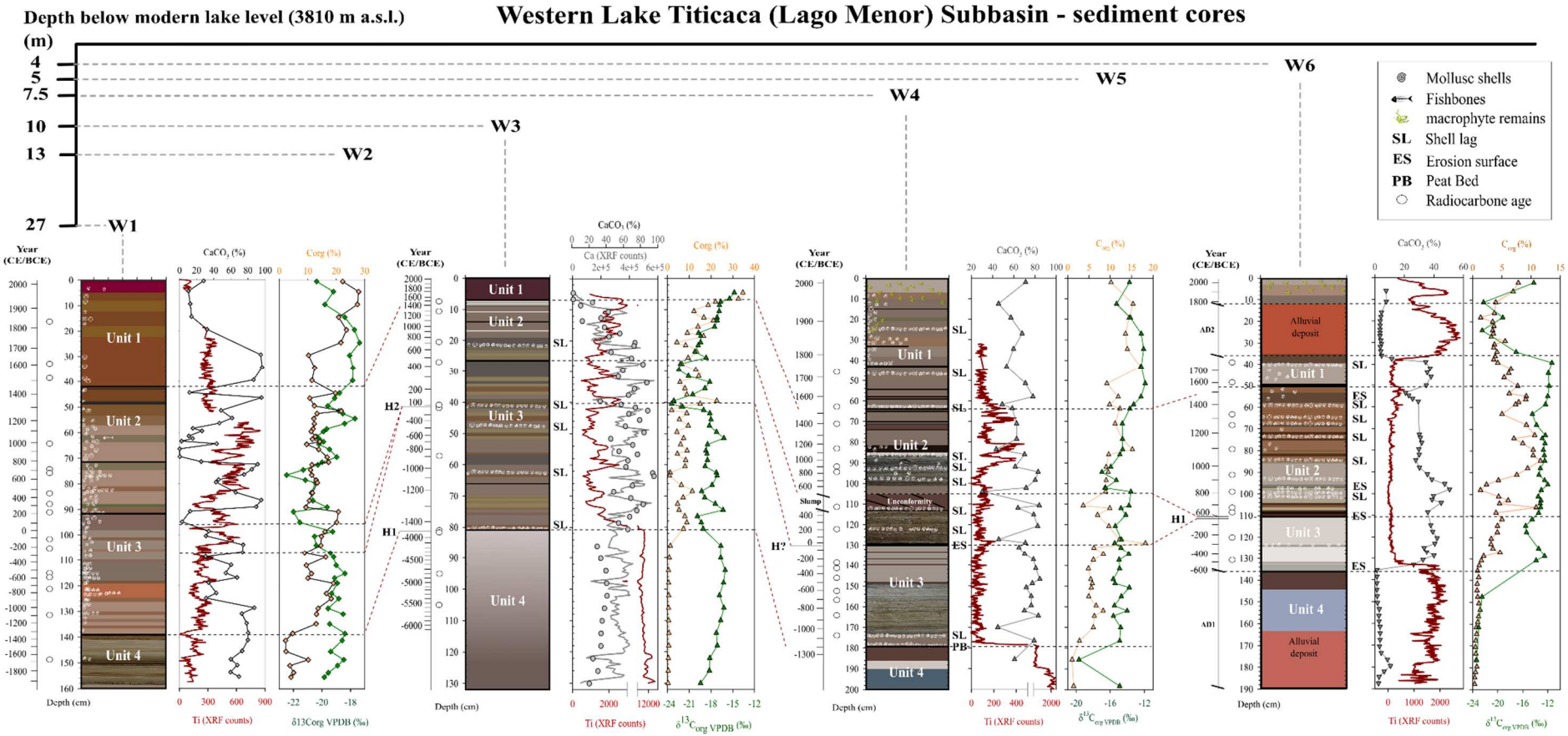

Fig. S3C: Sediment profiles from the western subbasin of Lago Menor, with their lithology and depth profiles of Ca, Ti, C_{org}, and $\delta^{13}C_{org}$ (uncorrected for the Suess effect). Lines indicate core scan XRF measurements, and symbols refer to chemical measurements. Temporal changes in lithology and sedimentation rate with water depth for the western part of the subbasin of Lago Menor corroborate observations made from the eastern one. The successive appearance of peat beds and organo-detrital sediment facies overlying gleyed soil layers (unit 4 in W4, W5, and W6) shows that the shallow water areas were gradually submerged between ~1300 and ~700 BCE. The major transgression of the lake during the 6th century did not cause major sediment erosion on the gentle slopes of the western Taraco trough (W3 and W4). Only the shallow water area (W6) exhibits a significant erosion surface (between~100 BCE to ~600 CE). An instantaneous deposit (turbidite) is recorded in the downstream core W4 for the same time period.

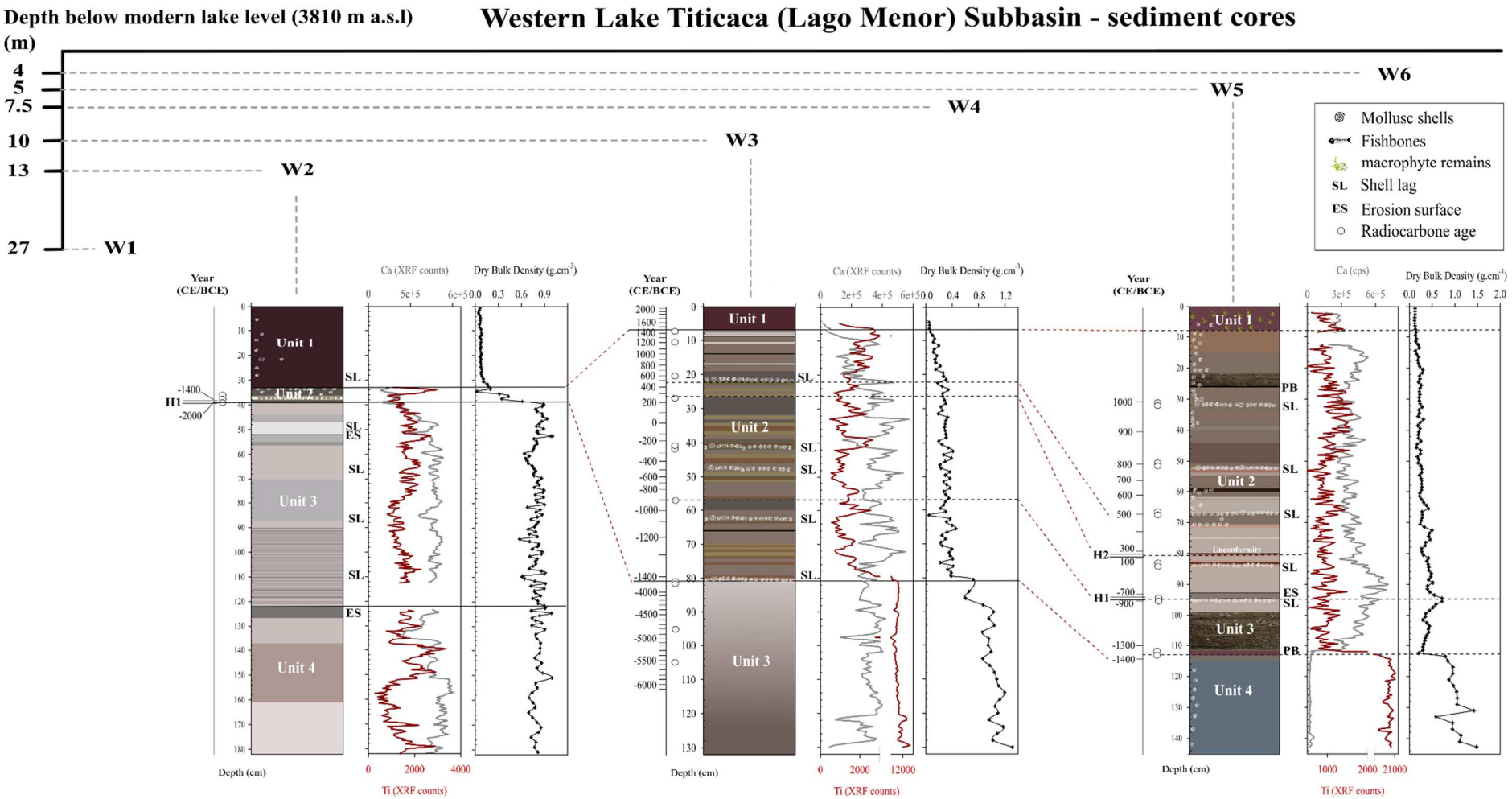

Fig. S3D: Sediment profiles from the western subbasin of Lago Menor, with their lithology and depth profiles of Ca, Ti, and dry bulk density (DBD) (uncorrected for the Suess effect). Lines indicate core scan XRF measurements, and symbols refer to chemical measurements. Abrupt decrease in DBD and Ti at around 1400 BCE illustrates the rapid filling of the southern subbasin (flooding of all areas 10 m or more below the modern level) after the Middle Holocene low stand (MLHS). At that time, areas 5 m or less below the modern level (e.g., W5 and W6) were covered by soils or peat and were subsequently flooded between 1300 and 700 BCE.

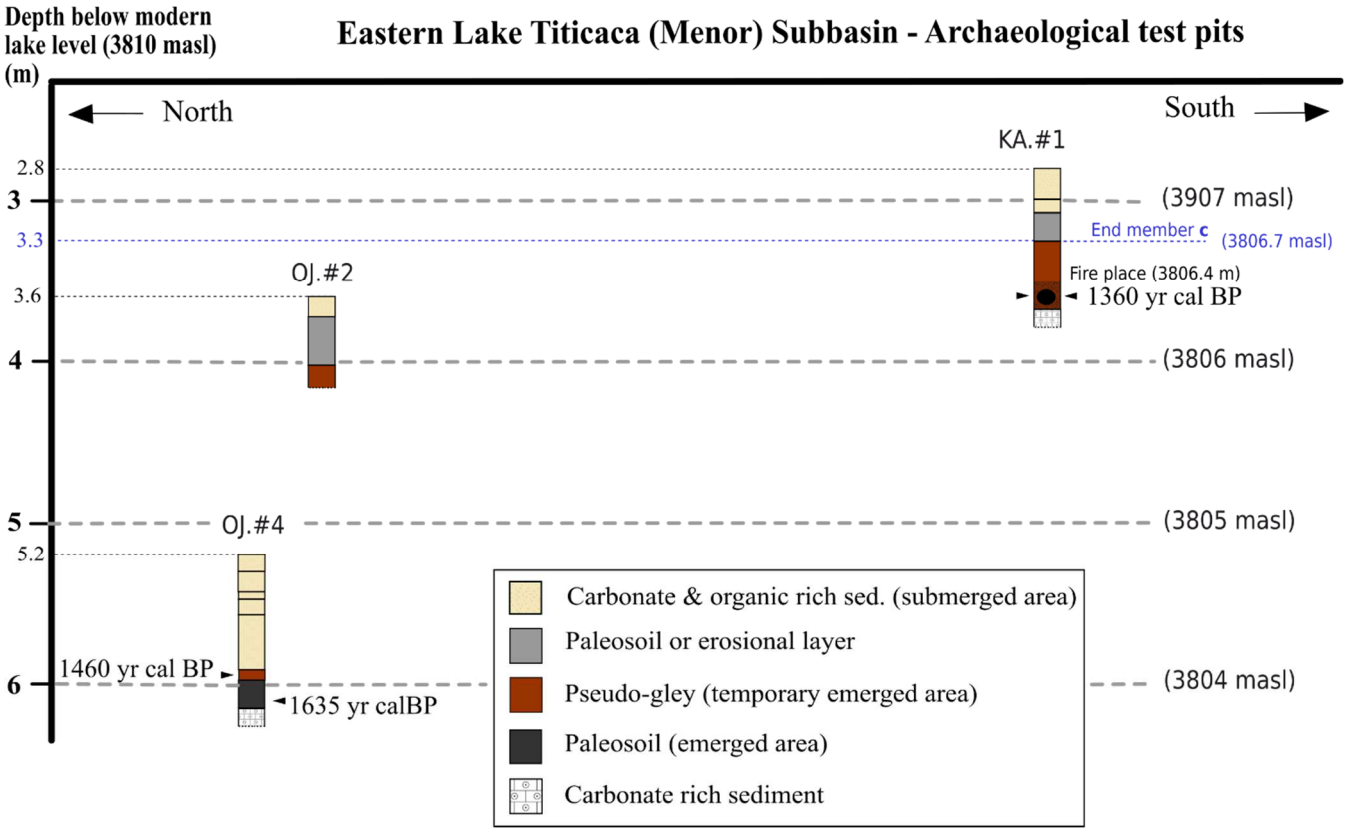

Fig. S3E: Archaeological test pit depth profiles at the sites of Ojelaya (OJ) and K'anaskia (KA) in the northeastern and in the southeastern part of Lago Menor with their lithology, and position of collected samples dated with radiocarbon. Charcoal ^{14}C dates obtained in test pits OJ.#4 and KA.#1 support that Lake Titicaca oscillated between 3804 and 3806.7 masl between 490 and 590 CE.

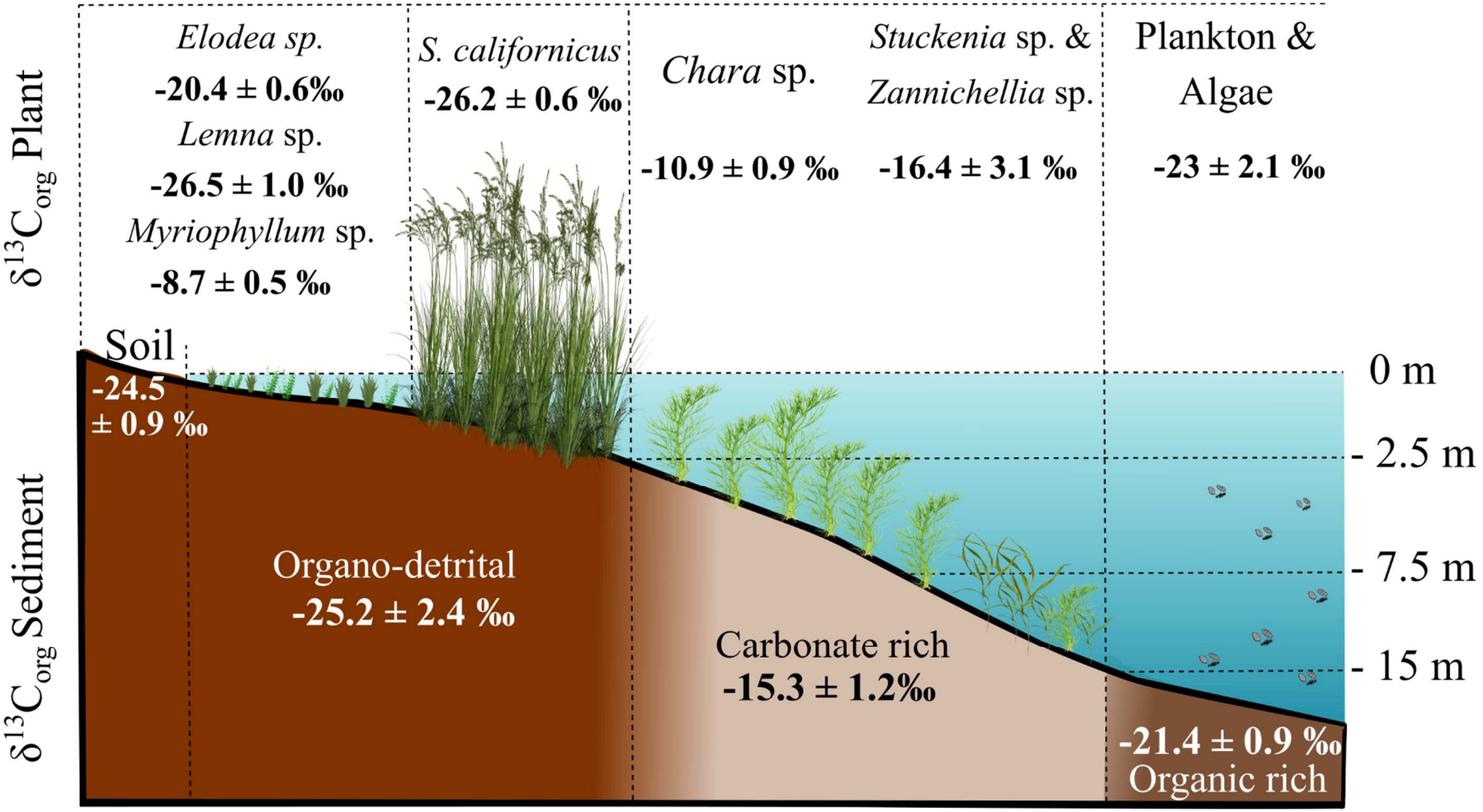

Fig. S4: Modern averaged values of $\delta^{13}C_{org}$ in soil, higher plants, macroalgae, phytoplankton/zooplankton and surface sediment along the slope of the southern subbasin of Lake Titicaca, summarized from this study and the literature (1-4). Values are not corrected for the Suess effect and are at least 2 ‰ lower than those before 1850 CE (32-34). All aquatic plants were collected in pristine areas unaffected by modern anthropogenic activities.

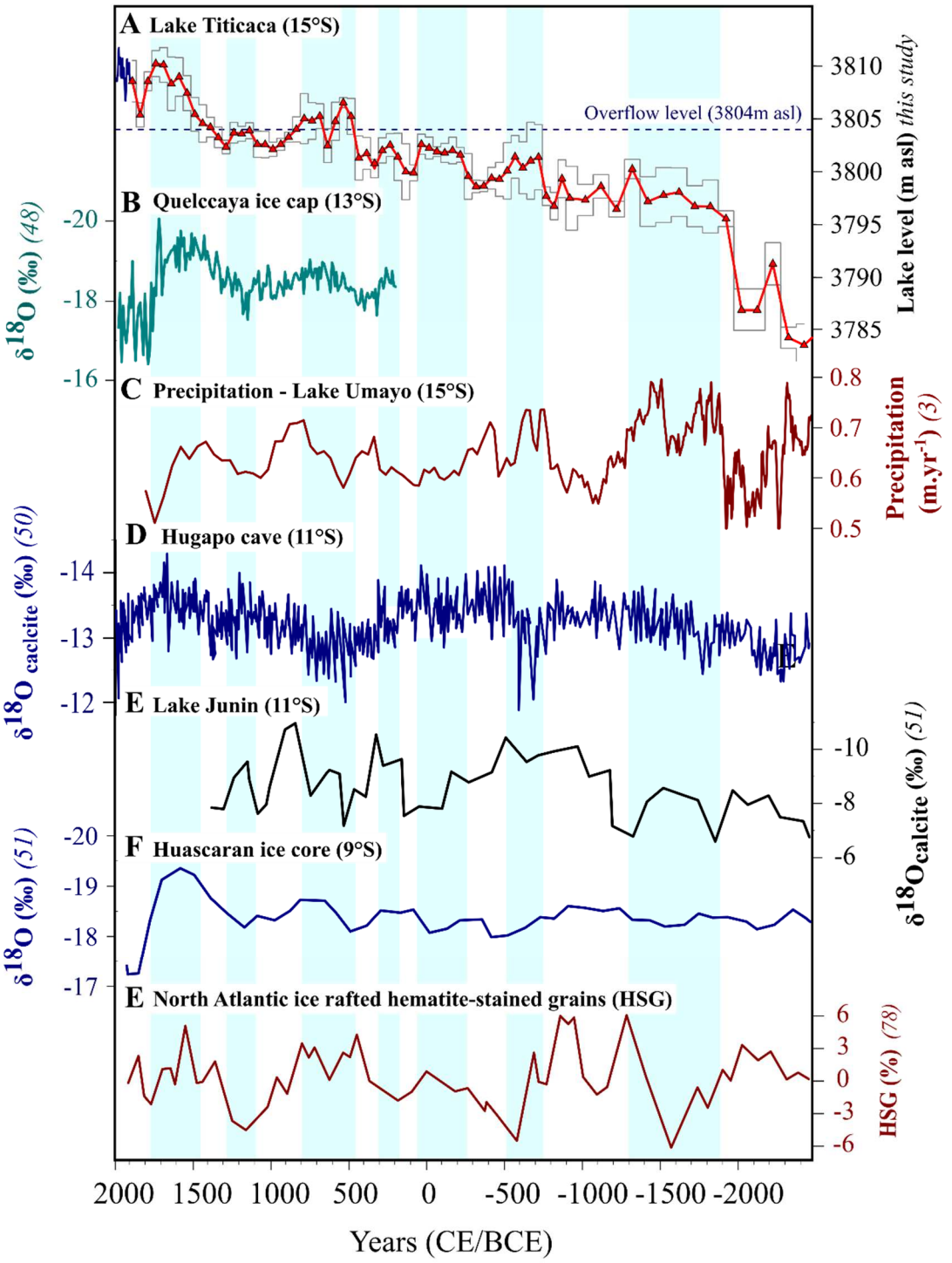

Fig. S5: A) Modeled averaged lake level curve obtained from the 10 cores collected in this study. B) Quelccaya ice cap $\delta^{18}O$ record (Peru) *(48)*. C) Reconstruction of precipitation from $\delta^{18}O$ in Lake Umayo (Peru) *(3)*. D) Huagapo cave speleothem $\delta^{18}O$ record (Peru) *(50)*. E) Lake Junin carbonate $\delta^{18}O$ record (Peru) *(51)*. F) Huascaran ice cap $\delta^{18}O$ record (Peru) *(51)*. E) North Atlantic ice rafted debris *(78)*. Note that Y axis for panels B, D, E and F are reversed, such that high values indicate wetter conditions and low values drier ones, for comparison with the inferred Lake Titicaca water level curve. Shaded blue background lines represent intervals of high or rising lake levels from the averaged modeled lake level curve.

Table S1: Modern $\delta^{13}C_{org}$ for plants, suspended organic matter, and surface sediment (0-1 cm) in Lake Titicaca from this study and other published studies *(5, 27, 28, 29)*.

Sample Type	Location	Plant Family (plant type over the sediment)	Plant type or sediment facies	average $\delta^{13}C_{org}$	SD	N	Water depth (m)	Reference
Plant	Lago Menor	Hydrocharitaceae	*Elodea* sp.	-20.4	0.6	2	< 1	1
Plant	Lago Menor	Haloragaceae	*Myriophyllum* sp.	-8.5	1.0	2	N.D.	2
Plant	Lago Menor	Haloragaceae	*Myriophyllum* sp.	-8.4	0.3	3	< 2	1
Plant	Lago Mayor	Haloragaceae	*Myriophyllum* sp.	-9.2	0.1	2	N.D.	4
Plant	Lago Menor	Cyperaceae	*Schoenoplectus totora*	-26.8	0.1	2	N.D.	2
Plant	Lago Menor	Cyperaceae	*Schoenoplectus totora*	-25.6	1.1	7	< 2	1
Plant	Lago Mayor	Cyperaceae	*Schoenoplectus totora*	-26.2	0.1	3	N.D.	4
Plant	Lago Menor	Characeae	Characeae	-11.6		1	N.D.	2
Plant	Lago Menor	Characeae	Characeae	-10.2	0.8	13	< 4	1
Plant	Lago Mayor	Potamogetonaceae	*Stuckenia* sp./*Zannichellia* sp.	-19.7	3.1	3	> 6	1
Suspended OM	Lago Mayor	Plankton/algae		-23.5	1.0		54 to 280	3
Suspended OM	Lago Mayor	pelagic organic matter		-26.5				4
Surface sediment (0-1)	Lago Mayor	Characeae and N.D.	Carbonate-rich sediment	-14.1	2.4	3	3 to 6	3
Surface sediment (0-1)	Lago Mayor	N.D.	Carbonate-rich sediment	-18.8	0.2	3	10 to 15	3
Surface sediment (0-1)	Lago Mayor	none / Hydrocharitaceae	Organo-detrital littoral sediment	-23.8	0.7	2	26	5
Surface sediment (0-1)	Lago Mayor	N.D.	Carbonate-rich sediment	-22.2	1.5		15 to 201	3
Surface sediment (0-1)	Lago Menor	Cyperaceae	Organo-detrital littoral sediment	-25.2	2.4	3	< 1.5	5 and 1
Surface sediment (0-1)	Lago Menor	Characeae	Carbonate-rich sediment	-15.3	1.2	5	3 to 13	5 and 1
Surface sediment (0-1)	Lago Menor	none (aphotic zone)	Organic-rich sediment	-21.4	0.9	5	28 to 41	5 and 1

Table S2A: Lake Titicaca sediment core information

Profile	Type	Sampling date	GPS coordinate	Profile length (m)	Lake level at sampling time (m)	Depth of sediment below 3810 m
E6	Gravity core	05/02/2015	S 16°12.57' W68°41.28'	0.73	3808.8	3.9
E5	Gravity core	16/05/2017	S16°12.329 W68°48.530	1.58	3807.9	5.6
E4	Gravity core	24/01/2017	S16°25.868 W68°80.894	1.58	3807.9	9.6
E3	Gravity core	24/01/2017	S16°23.359 W68°79.628	1.43	3807.9	30.4
E2	Gravity core	03/01/2014	S16°12.917" W68°46.113	1.61	3809.2	38.8
E1	Gravity core	24/01/2017	S16°19.991 W68°78.534	2.02	3807.9	43.1
W7	Gravity core	04/02/2015	S16°52710 W68°87196	1.88	3808.6	4.0
W6	Gravity core	10/03/2016	S16°52710 W68°87196	1.88	3808.6	4.0
W5	Gravity core	01/01/2014	S16º 21.628 W68º 51.459	1.44	3809.2	4.8
W4	Gravity core	10/03/2016	S16°5255 W68°89632	1.99	3808.6	7.3
W3	Gravity core	01/01/2014	S16º 21.458 W68º 52.817	1.31	3809.2	9.8
W2	Gravity core	01/01/2014	S16º 21.776 W68º 54.501	1.82	3809.2	12.8
W1	Gravity core	10/03/2016	S16°31231 W68°97081	1.56	3808.6	27.3

Table S2B: Lake Titicaca underwater archeological test pit information obtained at the site of Ok'e Supu *(22).*

Archeological test pits	Sampling date	Profile length (m)	Lake level at sampling time (m)	Lake bottom depth below 3810 masl
OKE-#1	06/2016	1.26	3808.5	1.7
OKE-#2	06/2016	0.92	3808.5	3.4
OKE-#3	06/2016	1.51	3808.5	8.2
OKE-#4	06/2016	0.81	3808.5	3.8
OKE-#6	06/2016	1.00	3808.5	5.15
OKE-#8	06/2016	0.77	3808.5	6.45
OKE-#9	06/2016	1.37	3808.5	3.05
OKE-#10	06/2016	1.44	3808.5	7.55
OKE-#11	06/2016	1.19	3808.5	2.9
OKE-#12	06/2016	0.87	3808.5	8.2
OKE-#13	07/2018	1.77	3808.2	3.4
OKE-#18	07/2018	0.42	3808.2	9.5

Table S3A: Unconformities or facies changes identified in sediment cores allowing end-member (EM) determination. EMt and EMb are the highest and lowest lake-level elevation end-members (with b as the bottom and t as the top), used for the construction of the modeled lake levels based on the TFCorg (Fig. 2). EM in parentheses are not used in the model but confirm the choice of selected end-members.

Core	Sediment Unit	Boundary	Depth in profile (m)	Upper age of boundary	Lower age of boundary	Lake bottom depth below 3810 masl	Sedimentary facies or context of the Unit	Estimated Lake level (m asl)	EMt	EMb
E5	U1	erosive surface (ES)	0.26	CE 1860	CE 1840	> 3803.5	Carbonate rich & shell lags	> 3803.5		(1)
W6	U1	AD 2		CE 1800	CE 1750	> 3804.9	Alluvial deposit	*3807.9*		
E4	U3	below slump	1.4	CE 1500	Undefined	> 3798.4	Carbonate rich	> 3801.4		(2)
E5	U2	hiatus (H2)	0.87	CE 1440	CE 1280	> 3802.9	Erosional or non-depositional	< 3802.9	b	
W5	U2	peat bed (PB)	0.25	CE 1300	CE 1250	< 3804.2	Peat bed	< 3804.2	(b)	
E5	U3/U4	hiatus (H1)	1.50 - 0.79	CE 1300	CE 780	> 3802.3	Finely laminated organo-detrital	> 3802.3		(2)
E5	U5	gleyed soil	1.98	~ CE 500		< 3801.8	soil layer	< 3801.8		
W4	U2	slump	1.05 - 1.13	CE 500		< 3800.8		> 3800.8		
W6	U2/U3	hiatus (H1)	1.07	CE 640	50 BCE	< 3804.2	Erosional or non-depositional	< 3804.2	d	
W5	U2	hiatus (H2)	0.82	CE 260	CE 100	< 3803.6	Erosional or non-depositional	< 3803.6	d	
W3	U1 to H2		0.21	modern	100 BCE	> 3799.3	Carbonate rich & shell lags	> 3799.3		3
W3	U3	hiatus (H2)	0.42	100 BCE	260 BCE	~ 3798.8	Erosional or non-depositional	> 3798.8		3

W5	U2	hiatus (H1)	0.96	520 BCE	840 BCE	< 3803.5	Erosional or non-depositional	< 3803.5	d	
W6	U4	gleyed soil	1.45-1.65	100 BCE	600 BCE	< 3803.6	soil layer	< 3803.6	d	
W5	U2	peat bed (PB)	1.12	1200 BCE	1240 BCE	< 3803.4	Peat bed above soil	< 3803.4	e	
W4	U3/U4	peat bed (PB)	1.8	1200 BCE	1240 BCE	< 3800.7	Peat bed above soil	< 3800.7	e	
W3	U3/U4	hiatus (H1)	0.82	1450 BCE	4000 BCE	<3798.3	Erosional or non-depositional	<3798.3		4
W2	U2/U3	hiatus (H1)	0.4	1400 BCE	2000 BCE	< 3796.1	Erosional or non-depositional	< 3796.1	f	
W1	U4		1.40	1800 BCE	1400 BCE	> 3780.5	Carbonate rich	*> 3783.5*		5
E3	U4	no		2400 BCE	1600 BCE	> 3778.2	Finely laminated organo-detrital	> 3778.2		5
W3	U4		0.82	4000 BCE	6000 BCE	> 3798.7	Carbonate rich	*> 3801.7*		6
E2	U4		0.67	5000 BCE	7000 BCE		Carbonate rich	3815	g**	

* obtained from age-depth model. Symbol < signifies that the lowest stratigraphic level identified in cores was below this altitude at the time indicated. Likewise, the > symbol indicates the highest stratigraphic level where lacustrine sediments are preserved, implying water level was above this point. ** Altitude of the shoreline at ca. 5000 BCE (3815 masl) derived from the literature (*40, 3, 77*). Estimated lake bottom depth (m asl) are only provided for shallow cores above 10 m and values presented in italic include the addition of an above water column typical of the sediment facies (e.g., 3m above carbonate rich facies).

Table S3B: Unconformities or facies changes identified in underwater archaeological test pits allowing end-member (EM) determination.

Test pit	Sediment Unit	Unconformity	Depth in profile (m)	Upper age of boundary	Lower age of boundary	Estimated water column (below 3810m asl)	Sedimentary facies of the Unit	EMt	EMb
OKE-#2	US1		0.06	CE 1791		> 3804.5	Carbonate rich & shell lags		1
OKE-#9	US2	Paleoshoreline	0.2	CE 1462		~ 3804.7	Sandy/erosional	b	
OKE-#4	US2	Paleoshoreline	0.16	CE 1385		~ 3804.0	Sandy/erosional	(b)	
OKE-#6	US2		0.28	CE 1472	CE 1436	> 3802.6	Detrital / Carb. rich		2
OKE-#8	US2		0.12	CE 1432		> 3801.4	Detrital / Carb. rich		2
OKE-#12	US2		0.13	CE 1392		> 3799.7	Detrital / Carb. rich		
OKE-#1	US3	Soil	0.46	CE 1196		< 3805.8		b	
OKE-#9	US3	Soil	0.44	CE 1114		< 3804.5		b	
OKE-#13	US3	Paleoshoreline	0.84	CE 1132		~ 3803.2	Sandy/erosional		
OKE-#2	US4		0.54	CE 1091		> 3804.1	Carbonate rich	b	
OKE-#12	US4		0.42	CE 1125		> 3799.4	Carbonate rich		(2)
OKE-#11	US5	Soil	0.66	CE 860		< 3804.4	Soil		
OKE-#9	US5	Soil	0.89	CE 849		< 3804.1	Soil		
OKE-#13	US6		1.36	CE 540		> 3802.6	Carbonate rich		2
OKE-#10	US6		0.68	CE 758		> 3799.8	Carbonate rich		2
KA		soil	0.80	CE 575	CE 530	< 3806.7	soil		c
OKE-#3	US8	Soil	1.51	273 BCE		< 3798.3	Soil		3
OKE-#5/7	US8		0.5	633 BCE		> 3794.7	Detrital / Carb. rich.		4

Table. S4: Radiocarbon dates and calibrated ages from Lake Titicaca sediment cores. Radiocarbon ages are calibrated using the most recent calibration curve (SHCal20). Rejected ages in bold. The calibrated ages before present (cal yr BP) 2σ range are presented at a 2σ probability interval including a 250 ^{14}C yr reservoir age for mollusc shells *(7)*.

Laboratory Code	Core ID	Depth in core (cm)	Sample type	Dating method	^{14}C age (yr BP)	Age 2σ range (yr cal BP)
OS-139248	W1	15.5	Mollusc shell	Hydrolysis - AMS	420 ± 20	21 - 73
OS-131438	**W1**	**31.5**	**Mollusc shell**	**Gas Bench**	**540 ± 120**	
OS-136697	W1	37.5	Mollusc shell	Gas Bench	570 ± 80	56 - 453
OS-136698	W1	58.5	Mollusc shell	Gas Bench	1100 ± 85	553 - 802
OS-136699	W1	63.5	Mollusc shell	Gas Bench	1340 ± 85	734 - 1057
IRPA T4 -74	W1	74	Mollusc shell	Hydrolysis - AMS	1735 ± 26	1179 - 1215
OS-131439	W1	74.5	Mollusc shell	Gas Bench	1680 ± 120	962 - 1428
OS-131440	W1	83.5	Mollusc shell	Gas Bench	2230 ± 120	1534 - 2115
OS-131441	**W1**	**88**	**Mollusc shell**	**Gas Bench**	**1280 ± 120**	
OS-131442	W1	90.9	Mollusc shell	Gas Bench	1920 ± 120	1276 - 1739
OS-131443	**W1**	**102.5**	**Mollusc shell**	**Gas Bench**	**2240 ± 120**	
OS-131444	W1	105.4	Mollusc shell	Gas Bench	2510 ± 120	1870 - 2439
OS-131445	W1	115.3	Mollusc shell	Gas Bench	2740 ± 130	2287 - 2751
IRPA T4 -103	W1	117	Mollusc shell	Hydrolysis - AMS	2835 ± 26	2493 - 2601
OS-131446	**W1**	**121**	**Mollusc shell**	**Gas Bench**	**2900 ± 120**	
OS-131447	W1	131	Mollusc shell	Gas Bench	3390 ± 120	2877 - 3487
OS-131448	W1	148.8	Mollusc shell	Gas Bench	3660 ± 120	3320 - 3892
OS-111084	W2	37.5	Mollusc shell	Gas Bench	3390 ± 95	3052 - 3467
OS-111085	W2	38.5	Mollusc shell	Gas Bench	3600 ± 95	3356 - 3775
OS-111086	W2	39.5	Mollusc shell	Gas Bench	3850 ± 95	3961 - 4443
OS-122401	W3	7.5	Mollusc shell	Gas Bench	855 ± 95	439 - 664
OS-122402	W3	10.5	Mollusc shell	Gas Bench	915 ± 95	503 - 692
OS-122403	W3	20.5	Mollusc shell	Gas Bench	1980 ± 100	1373 - 1756
OS-122404	W3	27.5	Mollusc shell	Gas Bench	2060 ± 100	1472 - 1897
OS-111087	**W3**	**41.5**	**Mollusc shell**	**Gas Bench**	**2070 ± 95**	
OS-111088	W3	42.5	Mollusc shell	Gas Bench	2420 ± 95	1512 - 1926
OS-122405	W3	56.5	Mollusc shell	Gas Bench	3080 ± 100	2742 - 3172
OS-111089	W3	80.5	Mollusc shell	Gas Bench	3450 ± 95	3144 - 3591
OS-111090	W3	81.5	Mollusc shell	Gas Bench	3470 ± 95	3165 - 3636
OS-122406	W3	94.5	Mollusc shell	Gas Bench	6210 ± 140	6443 - 7075
OS-122407	W3	115	Mollusc shell	Gas Bench	7740 ± 140	7960 - 8558
OS-136681	W4	45.5	Mollusc shell	Gas Bench	555	54 - 333
OS-136682	W4	63.8	Mollusc shell	Gas Bench	690 ± 85	277 - 531
OS-136683	W4	71.0	Mollusc shell	Gas Bench	890 ± 85	452 - 668
OS-136684	W4	83.5	Mollusc shell	Gas Bench	1120 ± 80	625 - 813
OS-136685	W4	92.0	Mollusc shell	Gas Bench	1460 ± 80	903 - 1178
SacA-57991	W4	94.5	Mollusc shell	Hydrolysis - AMS	1615 ± 30	1176 - 1273
OS-136686	**W4**	**110.8**	**Mollusc shell**	**Gas Bench**	**2090 ± 85**	
OS-136687	W4	122.5	Mollusc shell	Gas Bench	2100 ± 85	1510 - 1881
SacA-57992	W4	**137.3**	**Mollusc shell**	**Hydrolysis-AMS**	**610 ± 30**	
OS-136688	W4	141.5	Mollusc shell	Gas Bench	2650 ± 90	2098 - 2539
OS-136689	W4	146.8	Mollusc shell	Gas Bench	2760 ± 85	2318 - 2737
OS-136690	W4	152.8	Mollusc shell	Gas Bench	2910 ± 90	2362 - 2794
OS-136691	**W4**	**157.0**	**Mollusc shell**	**Gas Bench**	**2810 ± 85**	
OS-139820	**W4**	**164.5**	**Mollusc shell**	**Gas Bench**	**2100 ± 100**	

OS-139821	W4	176.5	Mollusc shell	Gas Bench	3290 ± 120	2846 - 3379
OS-111091	W5	31.5	Mollusc shell	Gas Bench	1300 ± 90	718 - 987
OS-111092	**W5**	**32.5**	**Mollusc shell**	**Gas Bench**	**1210 ± 90**	
OS-111093	W5	51.5	Mollusc shell	Gas Bench	1500 ± 95	958 - 1289
OS-111094	W5	52.5	Mollusc shell	Gas Bench	1470 ± 90	956 - 1273
OS-111095	W5	66.5	Mollusc shell	Gas Bench	1810 ± 95	1272 - 1611
OS-111096	W5	67.5	Mollusc shell	Gas Bench	1800 ± 95	1269 - 1590
OS-111097	W5	84.5	Mollusc shell	Gas Bench	2050 ± 95	1468 - 1888
OS-111098	W5	85.5	Mollusc shell	Gas Bench	2190 ± 90	1611 - 2016
OS-111099	W5	95.5	Mollusc shell	Gas Bench	2720 ± 95	2315 - 2745
OS-111100	W5	96.5	Mollusc shell	Gas Bench	2970 ± 95	2681 - 3063
OS-111101	W5	112.5	Mollusc shell	Gas Bench	3400 ± 95	3061 - 3492
OS-111102	W5	113.5	Mollusc shell	Gas Bench	3080 ± 110	2729 - 3212
OS-131423	W6	39	Mollusc shell	Gas Bench	480 ± 120	0 - 328
OS-131424	W6	48	Mollusc shell	Gas Bench	595 ± 120	56 - 495
OS-136692	W6	63	Mollusc shell	Gas Bench	1020 ± 80	533 - 731
OS-131425	W6	68	Mollusc shell	Gas Bench	1230 ± 120	634 - 985
OS-131426	W6	79.5	Mollusc shell	Gas Bench	1070 ± 120	554 - 920
OS-136693	W6	91	Mollusc shell	Gas Bench	1340 ± 85	734 - 1057
OS-131427	W6	98	Mollusc shell	Gas Bench	1570 ± 120	923 - 1320
OS-131428	W6	106	Mollusc shell	Gas Bench	1790 ± 120	1176 - 1584
OS-136857	W6	108.5	Mollusc shell	Hydrolysis - AMS	2360 ± 20	1896 - 1905
OS-137278	W6	108.5	Wood	ABA - AMS	1960 ± 20	1824 - 1923
OS-131429	W6	120.5	Mollusc shell	Gas Bench	2490 ± 130	1825 - 2465
OS-131430	W6	130.75	Mollusc shell	Gas Bench	2770 ± 130	2293 - 2759
SacA-57986	E1	19.5	Mollusc shell	Hydrolysis - AMS	635 ± 30	353 - 448
SacA-150675	E1	24.5	Mollusc shell	Hydrolysis - AMS	675 ± 15	321 - 453
SacA-50403	E1	34.5	Mollusc shell	Hydrolysis - AMS	830 ± 30	510 - 559
SacA-57987	E1	49.5	Mollusc shell	Hydrolysis - AMS	1220 ± 30	787 - 920
OS-136641	E1	60.5	Mollusc shell	Gas Bench	1150 ± 80	669 - 923
OS-136642	E1	70.75	Mollusc shell	Gas Bench	1230 ± 80	716 - 961
OS-136643	E1	82	Mollusc shell	Gas Bench	1450 ± 80	928 - 1180
OS-136644	E1	93	Mollusc shell	Gas Bench	1390 ± 80	899 - 1177
OS-136645	E1	105	Mollusc shell	Gas Bench	1540 ± 80	1047 - 1299
SacA-57988	E1	113	Mollusc shell	Hydrolysis - AMS	1665 ± 30	1265 - 1314
IRPA28142.1.1	E1	133	Terrestrial OM	ABA - AMS	1820 ± 40	1347 - 1526
OS-136646	E1	135	Mollusc shell	Gas Bench	1970 ± 80	1404 - 1747
OS-136647	E1	151	Mollusc shell	Gas Bench	2220 ± 80	1701 - 2057
OS-136648	E1	169	Mollusc shell	Gas Bench	2460 ± 80	1999 - 2343
OS-136649	E1	186.5	Mollusc shell	Gas Bench	2670 ± 85	2304 - 2720
28124.1.1	E1	186.5	Mollusc shell	Hydrolysis - AMS	2178 ± 30	
OS-136650	E1	193.5	Mollusc shell	Gas Bench	2780 ± 85	2356 - 2744
OS-136651	E1	201	Mollusc shell	Gas Bench	3100 ± 85	3088 - 2156
SacA-57989	**E3**	**23.5**	**Mollusc shell**	**Hydrolysis-AMS**	**580 ± 30**	
IRPA CHB-26	E3	25.5	Mollusc shell	Hydrolysis - AMS	546 ± 25	148 - 217
OS-136652	E3	35	Mollusc shell	Gas Bench	570 ± 75	57 - 341
IRPA CHB-39	E3	35.5	Mollusc shell	Hydrolysis - AMS	711 ± 25	192 - 308
IRPA CHB-52	E3	52	Mollusc shell	Hydrolysis - AMS	730 ± 25	465 - 528
IRPA CHB-60	E3	60.5	Mollusc shell	Hydrolysis - AMS	1090 ± 25	672 - 738
OS-136653	E3	62	Mollusc shell	Gas Bench	1120 ± 80	654 - 921
IRPA CHB-66	E3	70	Mollusc shell	Hydrolysis - AMS	1294 ± 25	901 - 938
OS-136654	E3	77.75	Mollusc shell	Gas Bench	1670 ± 80	1176 - 1420
SacA-57990	**E3**	**83**	**Mollusc shell**	**Hydrolysis-AMS**	**3890 ± 30**	

OS-136655	E3	89.75	Mollusc shell	Gas Bench	3710 ± 85	3481 - 3891
IRPA CHB-86	E3	98.3	Mollusc shell	Hydrolysis - AMS	3616 ± 30	3687 - 3854
OS-136656	E3	110.75	Mollusc shell	Gas Bench	3910 ± 85	3696 - 4154
OS-136657	**E3**	**122**	**Mollusc shell**	**Gas Bench**	**3780 ± 85**	
OS-136658	**E3**	**133**	**Mollusc shell**	**Gas Bench**	**3850 ± 85**	
OS-136659	E3	137	Mollusc shell	Gas Bench	4040 ± 85	3901 - 4359
28205.1.1	E3	142	Mollusc shell	Hydrolysis - AMS	4171 ± 30	4226 - 4446
28135.1.1	E4	16.5	Mollusc shell	Hydrolysis - AMS	227 ± 25	
OS-136660	**E4**	**33**	**Mollusc shell**	**Gas Bench**	**460 ± 75**	
OS-136661	**E4**	**43.5**	**Mollusc shell**	**Gas Bench**	**450 ± 75**	
OS-136662	**E4**	**59**	**Mollusc shell**	**Gas Bench**	**500 ± 75**	
OS-136663	**E4**	**69.5**	**Mollusc shell**	**Gas Bench**	**460 ± 75**	
OS-136664	**E4**	**77**	**Mollusc shell**	**Gas Bench**	**460 ± 75**	
OS-136665	**E4**	**115**	**Mollusc shell**	**Gas Bench**	**525 ± 75**	
28176.1.1	**E4**	**128.5**	**Mollusc shell**	**Hydrolysis - AMS**	**240 ± 25**	
28176.1.2	**E4**	**128.5**	**Mollusc shell**	**Hydrolysis - AMS**	**686 ± 25**	
28176.1.3	**E4**	**128.5**	**Mollusc shell**	**Hydrolysis - AMS**	**735 ± 25**	
OS-136666	**E4**	**141**	**Mollusc shell**	**Gas Bench**	**430 ± 75**	
OS-136667	E4	155.5	Mollusc shell	Gas Bench	715 ± 75	208 - 398
OS-136668	**E5**	**11.6**	**Mollusc shell**	**Gas Bench**	**>Modern**	
SacA-50391	**E5**	**26.8**	**macrophytes**	**ABA - AMS**	**565 ± 30**	
SacA-50390	**E5**	**26.8**	**Mollusc shell**	**Hydrolysis-AMS**	**505 ± 30**	
SacA-50393	E5	40.25	macrophytes	ABA - AMS	560 ± 30	144 - 221
SacA-50392	E5	40.25	Mollusc shell	Hydrolysis - AMS	550 ± 30	145 -219
28018.1.1	E5	41.65	Mollusc shell	Hydrolysis - AMS	563 ± 25	150 - 215
OS-136669	E5	55.25	Mollusc shell	Gas Bench	370	142 - 223
SacA-57992	E5	62.2	Mollusc shell	Hydrolysis - AMS	610 ± 30	281 - 332
IRPA-OJ1-72	E5	78	Mollusc shell	Hydrolysis - AMS	745 ± 25	493 - 527
SacA-50395	E5	**83.05**	**macrophytes**	**ABA - AMS**	**790 ± 30**	
SacA-50403	E5	**83.05**	**Mollusc shell**	**Hydrolysis-AMS**	**760 ± 30**	
27974.1.1	E5	83.05	Mollusc shell	Hydrolysis - AMS	734 ± 45	624 - 684
IRPA-OJ1-78	E5	85	Terrestrial OM	ABA - AMS	875 ± 25	715 - 771
OS-136672	E5	88.2	Mollusc shell	Gas Bench	1180 ± 85	673 - 930
OS-136673	E5	**98.8**	**Mollusc shell**	**Gas Bench**	**1300 ± 80**	
IRPA-OJ1-95	E5	110	Mollusc shell	Hydrolysis - AMS	1339 ± 25	922 - 979
OS-136674	E5	117.3	Mollusc shell	Gas Bench	1350 ± 80	794 - 1109
OS-136675	E5	132.5	Mollusc shell	Gas Bench	1380 ± 85	877 - 1177
OS-136676	E5	**150.7**	**Mollusc shell**	**Gas Bench**	**1410 ± 80**	
28022.1.1	E5	150.7	Mollusc shell	Hydrolysis - AMS	1559 ± 25	1176 - 1272
OS-136677	E5	1577	Mollusc shell	Gas Bench	1600 ± 80	1058 - 1354
OS-136678	E5	1703	Mollusc shell	Gas Bench	1630 ± 80	1174 - 1372
OS-136680	E5	1868	Mollusc shell	Gas Bench	1640 ± 85	1174 - 1378
RICH-24167	KA	100	Charcoal	ABA - AMS	1524 ± 31	1307 - 1416
RICH-24811	OJ#4	75	Charcoal	ABA - AMS	1608 ± 26	1404 - 1530
RICH-24812	OJ#4	90	Charcoal	ABA - AMS	1760 ± 26	1564 - 1701

SI References

1. S. C. Fritz et al., Quaternary glaciation and hydrologic variation in the South American tropics as reconstructed from the Lake Titicaca drilling project. Quatern. Res. 68, 410-420 (2007).
2. A. P. Ballantyne, P. Baker, S. Fritz, B. Poulter, Climate-mediated nitrogen and carbon dynamics in a tropical watershed. J. Geophys. Res. Biogeosci. 116 (2011).
3. P. A. Baker et al., The history of South American tropical precipitation for the past 25,000 years. Science 291, 640-643 (2001).
4. P. M. Tapia, S. C. Fritz, P. A. Baker, G. O. Seltzer, R. B. Dunbar, A Late Quaternary diatom record of tropical climatic history from Lake Titicaca (Peru and Bolivia). Palaeogeogr., Palaeoclimatol., Palaeoecol. 194, 139-164 (2003).
5. S. L. Cross, P. A. Baker, G. O. Seltzer, S. C. Fritz, R. B. Dunbar, A new estimate of the Holocene lowstand level of Lake Titicaca, central Andes, and implications for tropical palaeohydrology. The Holocene 10, 21-32 (2000).
7. M. B. Abbott, M. W. Binford, M. Brenner, K. R. Kelts, A 3500 14C yr High-Resolution Record of Water-Level Changes in Lake Titicaca, Bolivia/Peru. Quatern. Res. 47, 169-180 (1997).
22. C. Delaere, S. Guédron, The altitude of the depths: use of inland water archaeology for the reconstruction of inundated cultural landscapes in Lake Titicaca. Wld. Archaeol. 52, 67-83 (2022).
27. S. Guédron et al., Diagenetic production, accumulation and sediment-water exchanges of methylmercury in contrasted sediment facies of Lake Titicaca (Bolivia). Sci. Total Environ. 723, 138088 (2020).
28. M. Miller, J. Capriles, C. Hastorf, The Fish of Lake Titicaca: Implications for Archaeology and Changing Ecology through Stable Isotope Analysis. J. Archaeol. Sci. 37, 317-327 (2010).
29. H. D. Rowe et al., Insolation, moisture balance and climate change on the South American Altiplano since the Last Glacial Maximum. Clim. Change 52, 175-199 (2002).
32. J. Dombrosky, A ~1000-year 13C Suess correction model for the study of past ecosystems. The Holocene 30, 474-478 (2020).
33. C. D. Keeling, The Suess effect: 13Carbon-14Carbon interrelations. Environ. Int. 2, 229-300 (1979).
34. H. E. Suess, "Natural radiocarbon and the rate of exchange of carbon dioxide between the atmosphere and the sea" in Nuclear processes in geologic settings, N. R. Council, Ed. (University of Chicago Press, Washington, DC, 1953), vol. 43, pp. 52-56.
40. M. Servant, S. Servant-Vildary, Holocene precipitation and atmospheric changes inferred from river paleowetlands in the Bolivian Andes. Palaeogeogr., Palaeoclimatol., Palaeoecol. 194, 187-206 (2003).
48. L. G. Thompson et al., Annually resolved ice core records of tropical climate variability over the past~ 1800 years. Science 340, 945-950 (2013).
50. L. C. Kanner, S. J. Burns, H. Cheng, R. L. Edwards, M. Vuille, High-resolution variability of the South American summer monsoon over the last seven millennia: insights from a speleothem record from the central Peruvian Andes. Quat. Sci. Rev. 75, 1-10 (2013).
52. G. Seltzer, D. Rodbell, S. Burns, Isotopic evidence for late Quaternary climatic change in tropical South America. Geology 28, 35-38 (2000).
77. M. Servant, J. C. Fontes, Les lacs quaternaires des hauts plateaux des Andes Boliviennes: Premieres interpretations paleoclimatiques. Cahiers ORSTOM. Série Geologie 10, 9-23 (1978).
78. G. Bond et al., Persistent solar influence on North Atlantic climate during the Holocene. Science 294, 2130-2136 (2001).